Annual Variation of the Diurnal Cycle of Outgoing Longwave Radiation

BRANT LIEBMANN AND ARNOLD GRUBER*

Cooperative Institute for Climate Studies, University of Maryland, College Park, Maryland

(Manuscript received 1 September 1987, in final form 4 February 1988)

ABSTRACT

The annual variation of the diurnal cycle of outgoing longwave radiation (OLR) is examined. Our results are based on the climatological amplitude and phase of the first diurnal harmonic for each month. The diurnal harmonic was extracted from a composite daily cycle from several polar orbiting satellites that flew in different years with ten different equator crossing times. We compute a "diurnal vector standard deviation" which is the square root of the sum of the variances of both components of the 12 climatological monthly diurnal vectors. This allows contributions from both phase and amplitude changes of the diurnal vector.

A map of the diurnal vector standard deviation is presented. The values over land are an order of magnitude larger than over the ocean. The maxima are located over the seasonally migrating monsoons and over the midlatitude semi-arid zones. In midlatitudes the large standard deviation results from an increased daily cycle of insolation during summer and from clouds associated with midlatitude storms which reduce the diurnal cycle during winter. In the tropical monsoon regions a large variability of the diurnal cycle results from a larger daily cycle of cloudiness during the wet season than in the dry season. At some locations over the monsoons, however, the diurnal amplitude is actually a minimum during the wet summer season. We believe the minimum is caused by the pervasive cloudiness in the most convective regions. In the midlatitudes and during the dry season in the tropics, the maximum emission generally occurs between 1200 and 1400 local time. During the rainy season it occurs between 0600 and 0900.

We hypothesize that there should be a spatial relationship between the diurnal cycle variability and the standard deviation of the 12 climatological monthly means of OLR, and we compare maps of the two quantities. The large-scale features are in broad agreement and the correlation between the two maps is marginally statistically significant. A detailed comparison, however, reveals that the diurnal vector standard deviation is of much smaller scale than the standard deviation of OLR. We attribute the regional structure of the diurnal cycle variability to varying geography, vegetation, and available moisture. Some of the small-scale structure, however, undoubtedly arises because the diurnal cycle involves day–night differences which are inherently more noisy than the OLR field itself.

1. Introduction

The diurnal variability of outgoing longwave radiation (OLR) is still not well understood. Knowledge of the diurnal cycle is useful because of its obvious importance to the earth's radiation budget. OLR is also commonly used as a proxy for latent heat release in the tropics. Since tropical latent heat release is the primary driving mechanism of the tropics and is believed to affect midlatitude circulation, a better understanding of its diurnal cycle is relevant to atmospheric dynamics.

Although a conceptually simple measurement, documentation of the diurnal cycle is elusive because polar orbiting satellites make only two passes over a given point each day, and spatial coverage by geostationary satellites is incomplete. Hartmann and Recker (1986) and Gruber and Chen (1988) attempted to circumvent the problem of inadequate temporal coverage by polar orbiting satellites by compositing data from several satellites, which flew in different years with different equator crossing times. Hartmann and Recker were able to extract the first harmonic of the diurnal cycle of OLR and presented maps indicating phase and amplitude. Over dry land areas they found a maximum in longwave emission at noontime and attributed it to a daytime warming of the surface. Over convective land areas in the tropics the diurnal cycle is relatively small, but still larger than over the oceans. There are some significant amplitudes of the diurnal cycle, however, that occur in the areas of convection over the open ocean (Hartmann and Recker 1986; Albright et al. 1985). Gray and Jacobson (1977) pointed out that while the diurnal variability may be small over the ocean on scales large enough to be resolved by satellite, individual cumulonimbus undergo a strong diurnal cycle.

* Co-affiliation: National Environmental Satellite Data and Information Service, Washington, DC 20233.

Corresponding author address: Cooperative Institute for Research in Environmental Sciences, University of Colorado, Boulder, CO 80309-0449.

In this paper we study the annual variation of the diurnal vector of OLR. The difficulty in studying the variation of the diurnal cycle is that, since the vector varies in both amplitude and phase, no single number can completely describe its variability. Hartmann and Recker (1986) and Gruber and Chen (1988) compared maps of phase and amplitude for each of the seasons. In the present paper we compute a vector standard deviation which is a measure of both amplitude and phase changes of the climatological monthly mean diurnal vector over the course of the year. We also present time series at several gridpoints that show both the amplitude and phase of the diurnal vector.

2. Data

A series of sun-synchronous polar orbiting satellites with ten different equator crossing times flew nearly sequentially from June 1974 through December 1983. The primary equator crossings were at 0230, 0330, 0730, 0900 and 1200 local time. The different crossing times afford the opportunity to estimate the diurnal cycle. In the present study we use the calculations of Gruber and Chen (1988) of the climatological first diurnal harmonic for each month. Their estimates of the diurnal cycle compare favorably with those of other studies which utilized data from geosynchronous satellites.

Gruber and Chen first determined the mean flux for each month of the record for both day and night crossings at every gridpoint. Then they removed the day plus night average for that month. Thus, there are anomalies at two different hours for each month of the record of equal and opposite sign that are the result of the diurnal variability. This procedure eliminates calibration error of the instruments and is an attempt to remove interannual variability due to differences in the mean flux (see Liebmann (1987) for a discussion of potential problems associated with trying to remove the interannual variability). Since the two estimates for a given month are nearly twelve hours apart, there is little contribution from the second or higher even daily harmonics (Gruber and Chen 1988).

Data from the same month from different years with the same equator crossing times were then averaged. Data for the different equator crossing times were binned so that at every gridpoint there are estimates at ten different local times. The times were adjusted to account for the change of local crossing time with latitude. The data were then linearly interpolated to obtain an estimate at each hour. Finally, a Fourier analysis was performed that gives an estimate of the phase and amplitude of the climatological diurnal cycle for each month. Although Hartmann and Recker (1987) and Albright et al. (1985) gave examples of areas over the ocean where the second harmonic has significant amplitude, over most of the globe the diurnal variability is captured primarily by the first.

3. Results

a. *Large-scale patterns*

The standard deviation of a vector is defined as the square root of the sum of the variances of its components (Brooks and Carruthers 1953). The diurnal vector standard deviation can be expressed as

$$\sigma = \left(\frac{1}{12} \sum_{m=1,12} |\bar{\mathbf{V}} - \mathbf{V}_m|^2 \right)^{1/2}$$

where $\bar{\mathbf{V}}$ is the annual mean diurnal vector and $\mathbf{V}_m$ is the climatological mean diurnal vector for a given month. This definition permits both changes in amplitude and phase to contribute to the value of the standard deviation. For example, consider two diurnal vectors of equal magnitude, one with maximum amplitude at 0000 and the other at 0600. The usual calculation of scalar standard deviation based on amplitude alone would show zero standard deviation, but if the standard deviation were calculated as the root of the sum of the variances of both of its components, the result would be a large standard deviation at that point.

Figure 1a is a map of the diurnal vector standard deviation calculated from the 12 climatological monthly mean amplitudes and phases of the first diurnal harmonic. The zonal mean and twenty zonal harmonics are mapped which explain an average of 84 percent of the total variance on each latitude circle. The map is restricted to twenty harmonics because the field is noisy and we are presently interested in the large-scale features. Regional maps that have not been filtered are shown in part (b) of this section.

Even the smallest values of diurnal vector standard deviation over land are almost always larger than the largest values over ocean, and in general the values over land are an order of magnitude larger than those over water. The largest maxima occur over southern Africa and the semi-arid region of the Middle East. Lesser maxima are observed over southern North America, Brazil, across the sub-Sahara, over India, and over the western United States.

Hartmann and Recker (1986) and Gruber and Chen (1988) showed that during a given season the diurnal vector varies considerably between climatic regimes. Thus, a given location that undergoes a change over the course of a year (e.g., wet to dry or warm to cold) should have a large diurnal vector standard deviation. For example, India, which exhibits a large diurnal vector standard deviation (Fig. 1a), changes from a dry winter regime to an extremely wet summer monsoon.

A question arises as to whether the diurnal vector variability is a result of changes in amplitude of the diurnal cycle throughout the year or results from changes in the time of day of maximum emission. Figure 1b is a map of the standard deviation of the climatological diurnal cycle over the year based on

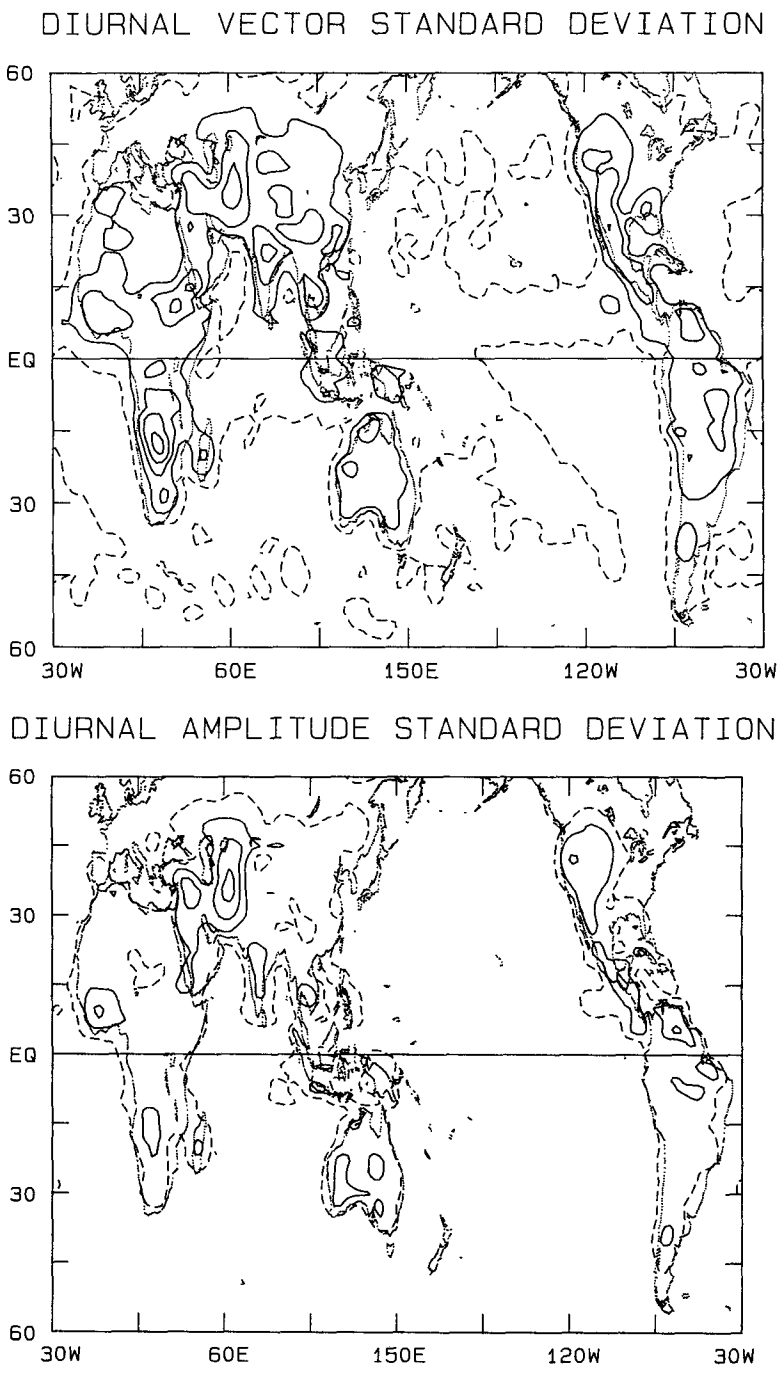

FIG. 1. (a) Amplitude of the diurnal vector standard deviation (defined in text) of outgoing longwave radiation (OLR) calculated from the 12 climatological monthly mean diurnal vectors. Dashed line is the 2 W m^{-2} contour. Solid contours start at 4 W m^{-2} with an interval of 2 W m^{-2}. The mean and first 20 zonal harmonics are plotted. (b) Amplitude of the diurnal cycle standard deviation based solely on the amplitude variation of the 12 climatological monthly mean diurnal cycles. Contours are the same as those in (a).

changes in amplitude alone. It is meant for comparison with Fig. 1a, which is a map of standard deviation based on changes of both amplitude and phase of the diurnal cycle. The plotted contours are the same on both maps. The standard deviation of amplitude alone can never exceed the vector standard deviation.

It is apparent that the maps are quite dissimilar, suggesting that phase changes contribute substantially to diurnal cycle variability. In particular, centers of variability over southern Africa, east central Africa, Asia, and North America are seen to be significantly larger on the vector standard deviation map (Fig. 1a) than on the amplitude standard deviation map (Fig. 1b). Also, areas of relatively large variability over the ocean relative to other oceanic areas on the vector variability map, such as the ITCZ and SPCZ, are absent on the amplitude variability map.

A map of the standard deviation of the 12 climatological monthly means of OLR is presented in Fig. 2. The 20 zonal harmonics contributing to this map contain on the average 97 percent of the variance on each latitude circle. Mean OLR is a measure of the temperature of the emitting surface (the cloud tops or the earth's surface). Therefore, a high standard deviation is indicative of regions that vary from clear to cloudy or warm to cold over the course of the year. Since these are the same areas that were previously described as having a large diurnal vector standard deviation, we expect to find a spatial correspondence between the two maps.

A visual comparison between the maps of OLR and diurnal vector standard deviation reveals that there are indeed many similarities. The centers over central South America are in nearly identical locations. The center of maximum OLR standard deviation west of Central America is over water where the diurnal vector variability is not expected to be large. There is a maximum in variability, however, relative to other oceanic areas.

Over Africa there are minor maxima in both diurnal vector and OLR standard deviation at the northern extreme of the migrating monsoon, and there are also maxima in both fields over southern Africa, with lobes extending eastward to Madagascar. A closer inspection of the centers over southern Africa, however, reveals that the peak in diurnal cycle variability is actually centered slightly poleward of the OLR standard deviation maximum, in a region of large OLR standard deviation gradient.

The great monsoon that migrates between northern Australia and India/southern Asia is not well defined on the diurnal vector standard deviation map because it is located over a mixture of land and ocean. There are peaks in diurnal vector standard deviation, however, over India, southern Asia, and northern Australia, which are the land areas with the largest OLR standard deviation associated with the monsoon. In the extratropics, maxima over the Middle East, southern South America, and the western United States coincide on both maps.

Figure 3a is a time series of climatological monthly means from a gridpoint at the centers of maximum diurnal vector standard deviation over the Middle East (Fig. 1a) and of standard deviation of OLR (Fig. 2).

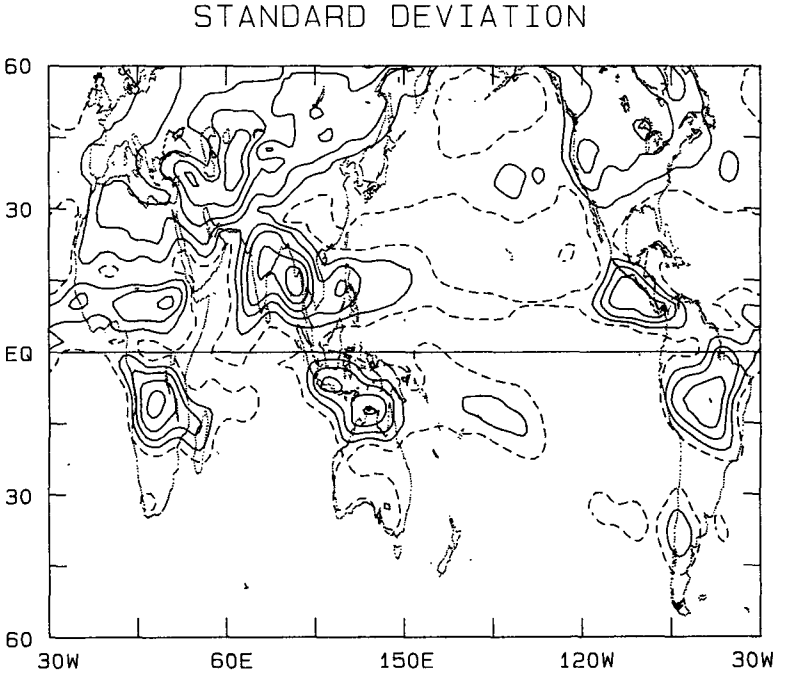

FIG. 2. Amplitude of the standard deviation of the 12 climatological monthly means of OLR. Contours begin at 10 W m^{-2} with an interval of 5 W m^{-2}. The 10 W m^{-2} contour is dashed. The mean and first 20 zonal harmonics are plotted.

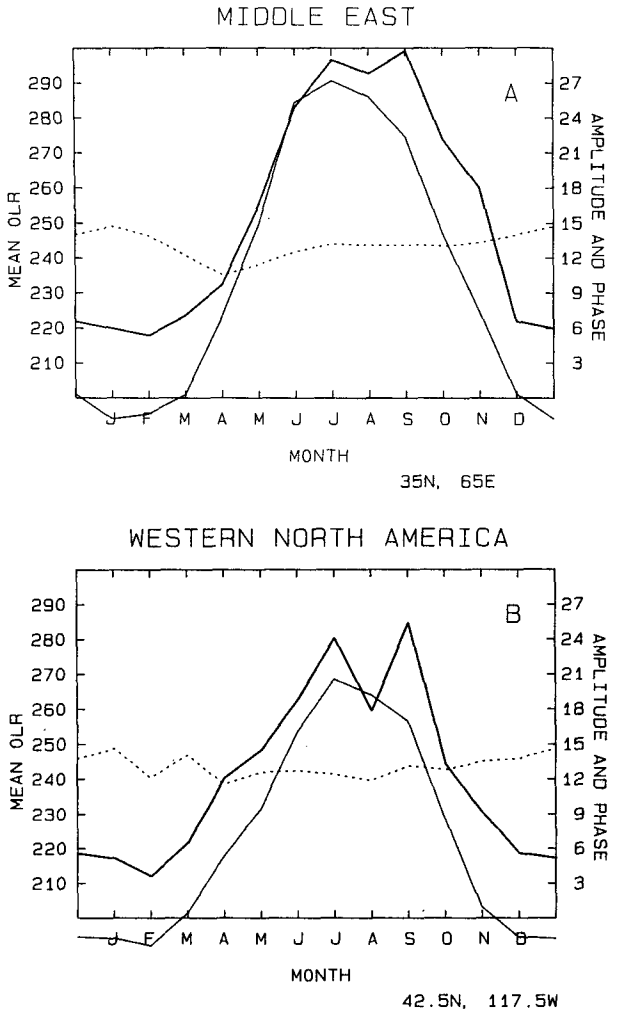

FIG. 3. Time series of the climatological monthly means of OLR (thin solid curve) in W m^{-2} (scale on left of diagram), the amplitude of the diurnal vector (heavy solid curve) in W m^{-2} (scale on right of diagram), and the time of maximum emission of the first harmonic (dashed curve) in local hours from 0 to 24 (scale on right of diagram). (a) gridpoint over Middle East centered at 35°N, 65°E; (b) gridpoint over western North America centered at 42.5°N, 117.5°W.

The scale on the left ordinate represents mean OLR, plotted as a thin solid curve, and the right scale represents amplitude and phase of the diurnal vector, plotted as heavy and dashed curves, respectively. The phase is plotted as the hour of maximum emission, and of course may never exceed 24. The time series is as one would intuitively expect from a semi-arid area. OLR is a maximum during summer; its annual cycle nearly parallels the amplitude of the diurnal vector. The time of maximum emission remains nearly constant between 1200 and 1500, responding to incident solar radiation.

Figure 3b is a similar curve corresponding to the center of maximum diurnal variability over the western United States. It exhibits the same characteristics as the curve at the middle east point. The occasional frontal passages and snow cover during winter may further reduce the diurnal vector and mean OLR during this season, increasing both the vector and OLR standard deviations. Gray and Jacobson (1977) noted, however, that the diurnal variation of deep cumulonimbus on scales smaller than our grid increases in the presence of organized synoptic systems.

The Amazon basin hosts one of the earth's great seasonal monsoons, and this is reflected in the maximum of both diurnal vector (Fig. 1a) and OLR standard deviation (Fig. 2). A time series of the gridpoint at 7.5°S, 50°W is presented in Fig. 4a. The OLR undergoes a large annual cycle, with the minimum occuring during the Southern Hemisphere summer rainy season. The diurnal cycle also exhibits a large change in amplitude between the dry and rainy season; it is largest during the wet season, apparently resulting from a large diurnal cycle in cloudiness. The change in diur-

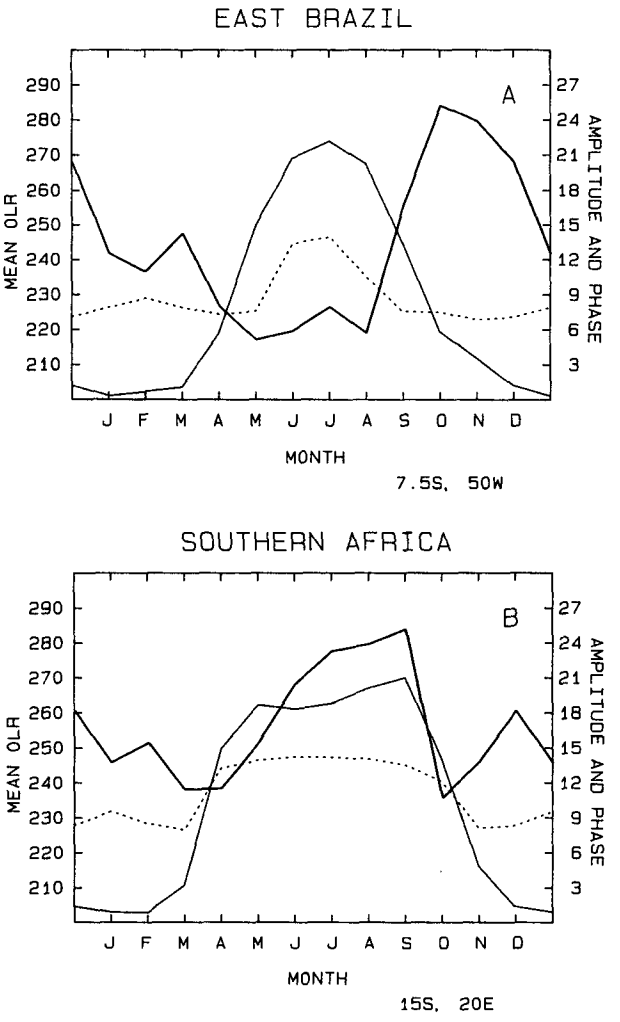

FIG. 4. As in Fig. 3 except gridpoint is over (a) eastern South America at 7.5°S, 50°W; (b) southern Africa at 15°S, 20°E.

nal amplitude through the year is only slightly less than over the semi-arid zones of the midlatitudes. The difference between the time series over the midlatitude semi-arid zones and those over the Amazon basin is that the maximum diurnal vector occurs with minimum mean OLR over the Amazon, but with maximum OLR over the midlatitude semi-arid regions.

The Amazon basin and most of the convective areas over land exhibit a similar phase variation. During the dry season the maximum emission is shortly after noon, as it is over the deserts, but during the rainy season it occurs between 0600 and 0900.

The area of maximum diurnal vector standard deviation over southern Africa is in dramatic contrast to the Amazon basin. Figure 4b is the time series at 15°S, 20°E, the center of maximum diurnal variability. It does not coincide with the maximum in OLR standard deviation. The mean OLR is a minimum during summer, suggesting convection during that part of the year. The phase also shifts nicely from a noontime maximum during the dry season to a morning maximum during the rainy season. The amplitude of the diurnal vector, however, is a maximum during the dry winter months. The Amazon basin (Fig. 4a) shows a strong maximum in diurnal variability during the wet season.

Although the largest diurnal cycle occurs at different times of the year over southern Africa and the Amazon basin, the rainfall patterns are actually quite similar. Porto Nacional, Brazil (10.5°S, 48.7°W) averages 12 mm rainfall during the three driest months and 880 mm during the three wettest months (Rastibona 1976). Mongu, Zambia (15°S, 23°E) averages 617 mm during the three wet months and very little during winter (Kendrew 1961). We attribute the different seasons that the maximum diurnal cycle occurs in the two regions to the differences in vegetation and available moisture. The Amazon basin is a damp tropical rainforest and during the dry season much of the insolation results in evaporation. During the dry season over southern Africa, however, the land is drier than over the Amazon basin and most of the insolation heats the surface, resulting in desert-like diurnal variability. A more detailed comparison with other regions in southern Africa, which behave more like the "usual" convective regions, is presented in part (b) of this section.

In the regions characterized by seasonal monsoons, the magnitude of the diurnal vector often decreases as the wet season progresses. This is true over the Amazon and also over India, which is represented by the gridpoint at 22.5°N, 80°E (Fig. 5). We believe that as convection becomes more established over the course of the wet season the clouds eventually persist the entire day. Therefore there is never a cloud-free satellite measurement, so the diurnal cycle decreases. Other locations over India exhibit a similar, but less well-defined, tendency for the diurnal cycle to decrease during the wet season.

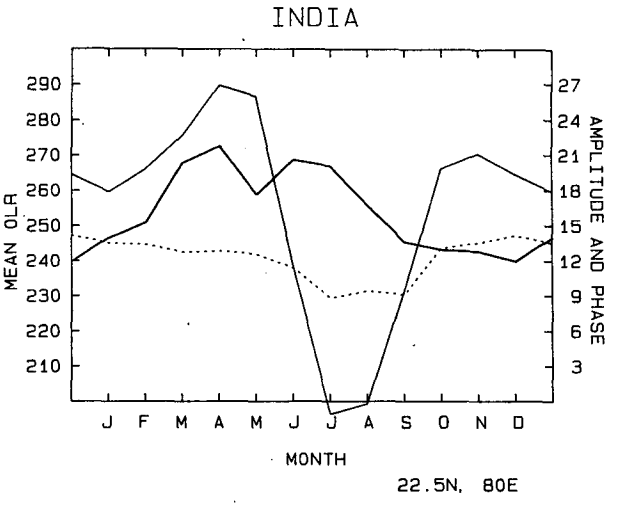

FIG. 5. As in Fig. 3 except gridpoint is over India at 22.5°N, 80°E.

b. *Regional patterns*

Since the diurnal cycle is related to the amount and type of cloud present, and since seasonal variations in cloud amount and type result in variations of mean OLR, we expect a relationship between large-scale patterns of the diurnal vector standard deviation and those of OLR. The time series (especially Figs. 3 and 4) and a visual comparison of the global maps of the quantities (Figs. 1 and 2) appear to support this claim. The correlation between the area weighted 20 harmonics of the diurnal vector and OLR standard deviations is 0.68. For the unfiltered fields the correlation is 0.65. The correlation increases as the number of zonal harmonics is reduced, supporting our claim of correspondence on large scales. While one must reject the null hypothesis at the 95 percent level for a correlation of 0.68 using a two-sided *t*-test if one assumes as few as seven degrees of freedom, it is nonetheless unsatisfying that the correlation is not somewhat larger. Furthermore, when separate correlations were calculated for "land" and "ocean" areas, the individual correlations decrease. The lesser correlations over ocean and land separately than for the map as a whole suggest that some of the correlation results from the generally large values of diurnal cycle variation over land and small values over the oceans. In this subsection we investigate some of the details of the diurnal vector standard deviation map and offer explanations as to why the diurnal vector and mean OLR standard deviations are often unrelated.

Figure 6a is an enlarged map of North and Central America on which the unfiltered diurnal vector standard deviation is plotted. Many of the features are too regional to appear on the global map. The corresponding map of OLR standard deviation (Fig. 6b) is smoother and quite unlike the diurnal vector standard deviation map. Although maxima are centered over

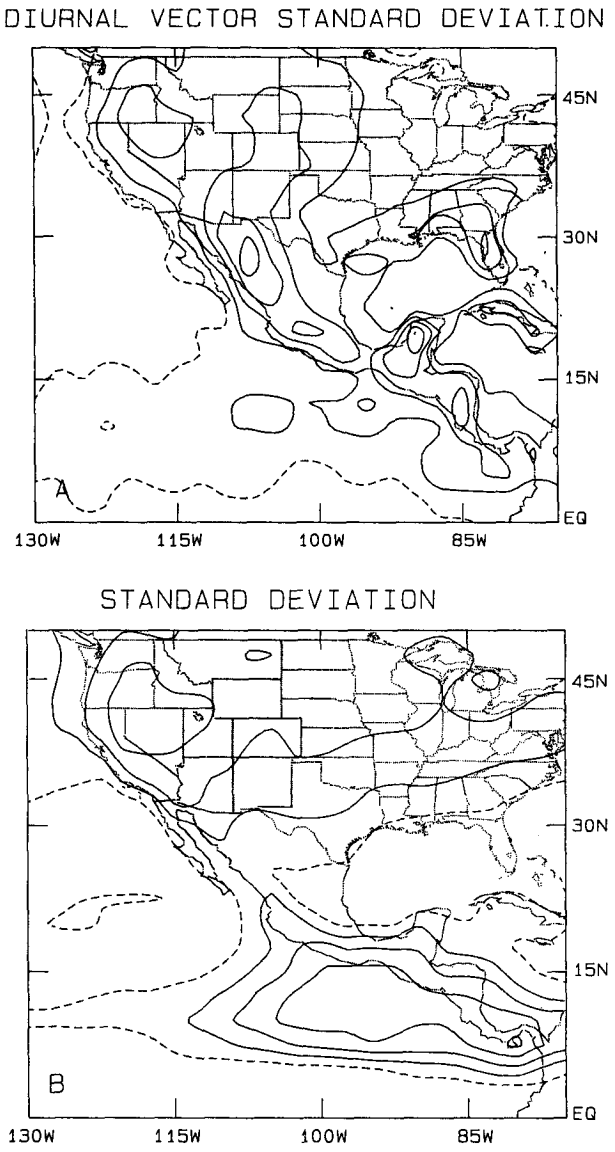

FIG. 6. (a) Unfiltered diurnal vector standard deviation over southern North America and Central America. Contours start at 2 W m^{-2} with an interval of 2 W m^{-2}. 2 W m^{-2} contour is dashed. (b) Unfiltered standard deviation of OLR. Contour interval is 5 W m^{-2} starting at 10 W m^{-2}. 10 W m^{-2} contour is dashed.

the western United States on both maps, the diurnal cycle variation maximums over Florida, Mexico, and the Yucatan Peninsula are not evident in OLR standard deviation.

The time series at the gridpoint of maximum diurnal vector standard deviation over the Yucatan Peninsula is shown in Fig. 7. The maximum in diurnal variability results from the contrast between a large diurnal cycle during the summer convective season and a small diurnal cycle during winter. The time series of the diurnal cycle is similar to that over eastern Brazil (Fig. 4a). There are two minima in mean OLR over the Yucatan. One minimum occurs as a result of convection during summer, and the other occurs during the cool winter months. The time series of the diurnal vector for the gridpoints of relative maxima over Florida and central Mexico (not shown) are similar to that over the Yucatan but are not as clearly defined.

The double minimum in mean OLR over the Yucatan, rather than a single cycle of large amplitude as over Brazil, results in a smaller standard deviation of OLR over the Yucatan (Fig. 6b) than Brazil (Fig. 2). We believe that the differences in mean OLR between the time series over the Yucatan Peninsula and Eastern Brazil result from different scales in the convection. The convection over the Yucatan is regional in extent, while the Amazon basin is the source of one of the great monsoons. Convection is so widespread over the Amazon that it results in a much lower mean OLR during the summer, hence a larger OLR standard deviation, than over the more regionally convective area, where rainfall is more scattered. Mean cloudiness statistics support this claim. Merida, Yucatan, Mexico receives most of its rainfall from June to September. The average cloudiness for those months is 60 percent (Aleman and Garcia 1974). Porto Nacional, Brazil, on the other hand, receives most of its rainfall from November to March. During these months the average cloudiness is 87.6 percent (Rastibona 1976). Additionally, the longer rainy season over the Amazon than over the Yucatan results in the annual cycle of mean OLR being dominant, while the shorter convective season over the Yucatan and other areas of regional convection, results in an important contribution from the semi-annual cycle.

The differences in scales of convection, then, offer a possible explanation of why the standard deviation

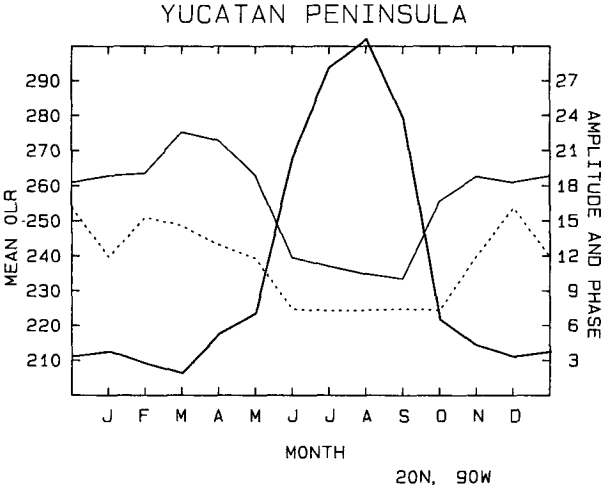

FIG. 7. As in Fig. 3 except the gridpoint is over the Yucatan Peninsula at 20°N, 90°W.

of OLR is a much smoother field than that of the diurnal vector. Only the largest scales of convection reduce the mean OLR sufficiently that a large enough minimum is produced during the rainy season to result in a large standard deviation of OLR. Over the Yucatan Peninsula the convection is more widely spaced, resulting in a higher mean OLR during summer and less standard deviation than over the Amazon.

The pattern of diurnal vector standard deviation also exhibits much small-scale variability over Africa which is not apparent in Fig. 1a. Figures 8a and 8b are maps of diurnal vector and OLR standard deviation over Africa. They have not been spatially filtered. Again the standard deviation of OLR is much smoother than that of the diurnal vector.

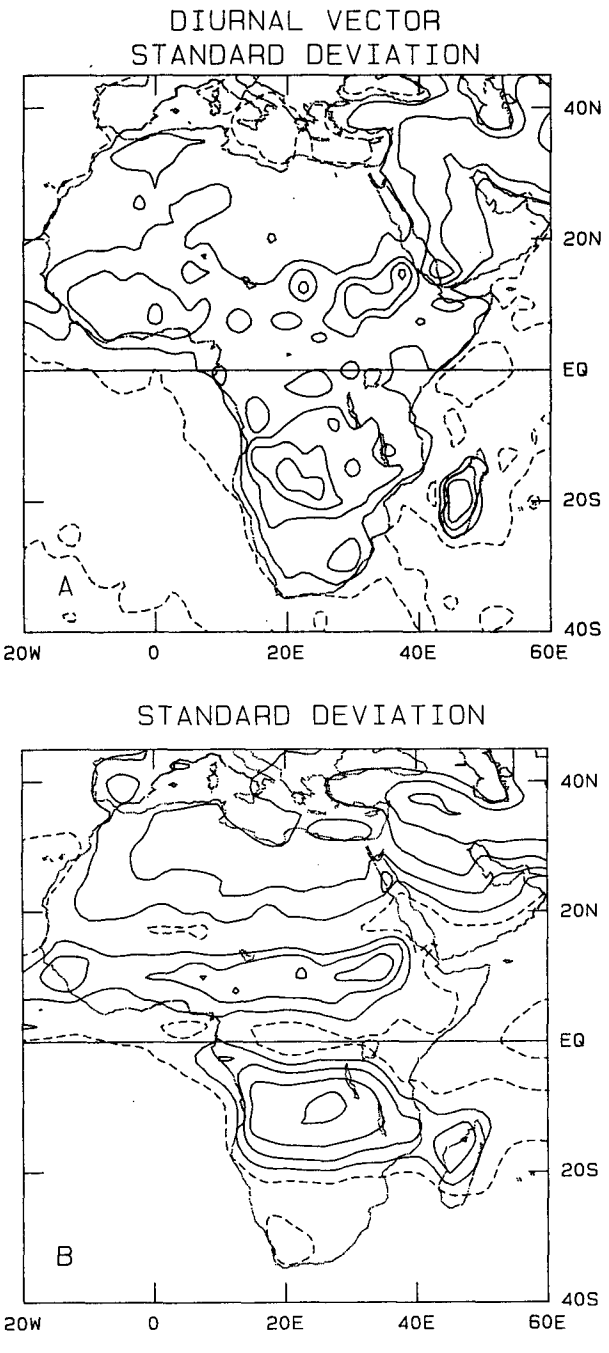

FIG. 8. As in Fig. 6 except over Africa.

The Sahara desert is not a region of large diurnal vector standard deviation, yet it contains a broad maximum of OLR standard deviation. Figure 9a is a time series of the point at 25°N, 20°E. While the mean OLR goes through a large annual cycle, the amplitude is less than over the Middle East (Fig. 3a) or the western United States (Fig. 3b). The amplitude of the diurnal vector is large all year, but increases only slightly during summer. We attribute the relatively small annual cycle and small variability of the diurnal vector over the Sahara to the fact that it is closer to the equator than the other arid regions. Thus there is less of an annual cycle of incident radiation than over the arid lands farther north. Also, the high clouds associated with midlatitude storms, which further reduce the mean OLR and the diurnal vector during winter, are absent over the Sahara.

Our result of a larger diurnal cycle over the Sahara during summer than winter is not inconsistent with the results of Duvel and Kandel (1985). They plotted diagrams of the number of pixels per radiance count versus time in different parts of the Sahara for three days each in January and August 1979, using METEOSAT data. They found that in the west Sahara (west of about 5°E), the average diurnal cycle is actually larger in January than July. In a box farther east, however, the January and July amplitudes are nearly equal. This is consistent with a diurnal cycle whose amplitude decreases in January with respect to July from west to east. Thus, since the time series depicted in Fig. 9a is at a gridpoint at the eastern edge of the later box, a larger diurnal cycle during summer than winter at this gridpoint is consistent the results of Duvel and Kandel (1985). Their results are also consistent with a time series at 25°N, 7.5°E (not shown), whose diurnal amplitude shows little change with season. Duvel and Kandel attributed the decreased diurnal cycle in August relative to January to an increase in atmospheric water vapor during August.

The pattern of diurnal cycle variability varies rapidly in southern Africa. We showed in part (a) of this section that the pattern at the center of maximum variation in diurnal variability is unlike any other monsoon region (Fig. 4b). To the northeast of that point, however, at the center of maximum OLR standard deviation (Fig. 8b), the time series more resembles other convective regimes. At this gridpoint (Fig. 9b) the OLR is lowest during summer, as it is at the point to the southwest. Unlike the point to the southwest, however, the amplitude of the diurnal cycle is slightly larger during summer, although it varies little throughout the year.

Time series over the island of Madagascar (Fig. 9c)

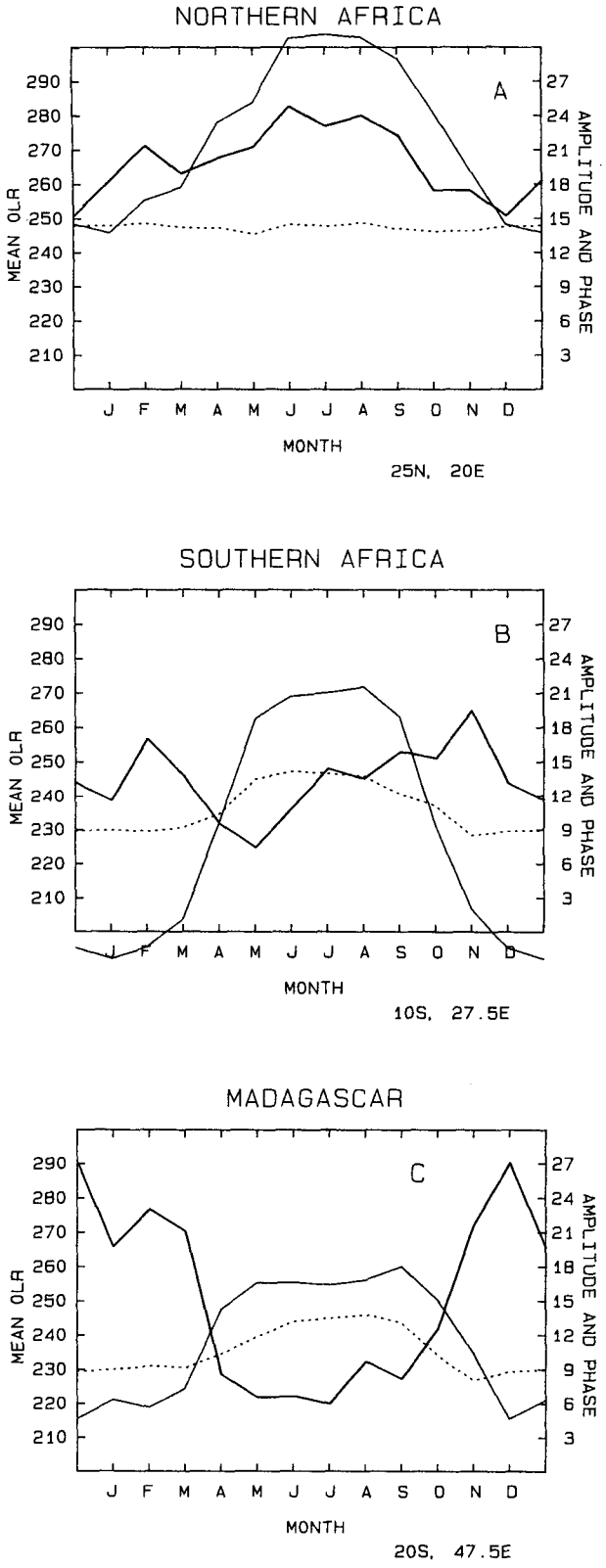

FIG. 9. As in Fig. 3 except (a) over North Africa at 25°N, 20°E; (b) over southern Africa at 10°S, 27.5°E; (c) over Madagascar at 20°S, 47.5°E.

look quite similar to the large-scale convective region over the Amazon (Fig. 4a). OLR is a maximum during winter, diurnal variability is largest during summer, and the time of maximum emission shifts from early afternoon during winter to midmorning in the wet summer.

There is a broad belt of scattered maxima in diurnal cycle variability across Africa, north of the equator (Fig. 8a). From time series of OLR it can be discerned that convection dominates the annual cycle, at least west of the Tanzanian–Ethiopian highlands, but the annual cycle of the diurnal variability is unclear. At many gridpoints it varies sporadically throughout the year, and there is no apparent preference for a maximum during the wet season.

The diurnal cycle standard deviation over South America (Fig. 10a) varies on regional scales, but the individual time series are relatively uniform over larger spatial scales than over Africa. Throughout the the Amazon basin the diurnal vector varies in a similar manner as at the point of maximum standard deviation over Brazil (Fig. 4a). There is actually a minimum in diurnal cycle standard deviation over the center of the basin. We attribute the minimum to cloudiness that is so widespread during the rainy season that it is always present. This reduces the amplitude of the diurnal cycle during that season, thus reducing its standard deviation.

North of the Amazon basin there is a band of increased diurnal vector standard deviation. A time series of the point of maximum variability is shown in Fig. 11. It is similar to other convective areas in that low OLR and a large diurnal vector are apparent in summer. The time of maximum emission, however, occurs around noon. In most of the other convective regimes it occurs in early to mid-morning.

The high diurnal vector standard deviation near the west central coast of South America is influenced by the Andes. The area of high standard deviation in southern South America behaves like the arid regions of the midlatitudes discussed earlier.

c. The oceans

The diurnal vector variability over the ocean is relatively small compared to that over land. This results from a relatively small diurnal vector over the ocean (Hartmann and Recker 1986; Gruber and Chen 1988). Even if there are large fractional changes in amplitude or large changes in phase of the diurnal vector over the ocean, the total vector change must be small. Compared to other oceanic areas the diurnal vector is relatively large over the Pacific ITCZ, although it appears to vary in latitude with season. The diurnal vector is also large over the SPCZ during the December, January February season (Hartmann and Recker 1986; Albright et al. 1985). The vector standard deviation map (Fig. 1a) reveals a band of maxima across the Pacific between 5° and 15°N with an extension southeastward from

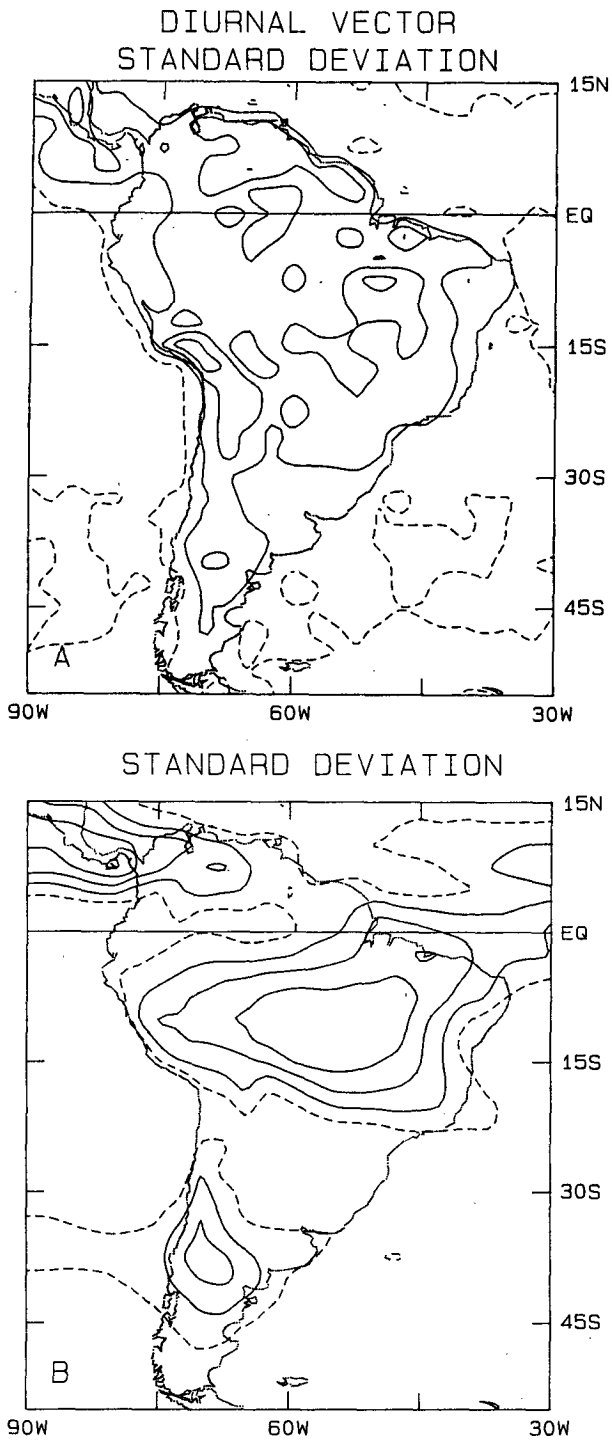

FIG. 10. As in Fig. 6 except over South America.

the western Pacific into the SPCZ. A band of high diurnal vector standard deviation also stretches across the Atlantic at the latitude of the ITCZ.

The oceanic areas west of the Southern Hemisphere continents have a large diurnal vector compared to most of the tropical ocean (Hartmann and Recker 1985), yet the diurnal vector standard deviation map (Fig. 1a) insists that there are distinct minima in each of the three regions. The minima west of Africa and South America extend from the stratus regions off the coast, characterized by high albedos, to the clear oceanic highs. Thus despite the relatively large diurnal vector west of the Southern Hemisphere continents, the vector is nearly constant throughout the year.

It is impossible to pick a time series to characterize all oceans. The diurnal vector is usually small and the amplitude and phase vary in a seemingly random fashion throughout the year. The most robust spatial pattern occurs near the northwest coast of Central America. There is a relatively large diurnal vector variability here compared to other ocean areas (Fig. 6a) and a large OLR standard deviation (Fig. 6b). This is an area that is characterized by heavy precipitation during summer as the monsoon moves northward. Figure 12 is a time series over the Pacific Ocean at 5°N, 82.5°W. It shows the maximum diurnal vector during the rainy season, with maximum emission between 0300 and 0500.

It is not clear that this point is entirely free from the influence of land. Reed and Jaffe (1981) suggested that in the eastern Atlantic the large diurnal cycle away from the coast is influenced by the continent. Further to the west the signal diminishes considerably.

The signal is weak over the western Pacific as well. This region is characterized by abundant rainfall during Northern Hemisphere winter months. If a significant land mass lies beneath the gridpoint in question, however, the time series behaves like most of the convective areas over land.

In contrast to the results of the present study, which indicate that there is little diurnal cycle over the open ocean, several other authors have found a large oceanic diurnal cycle. Houze et al. (1981) found a regular diur-

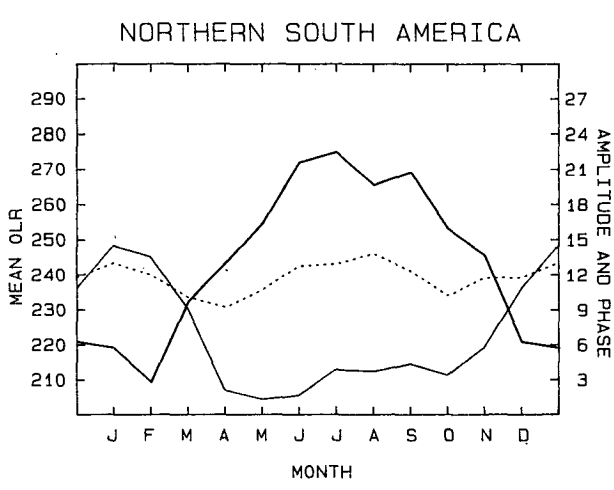

FIG. 11. As in Fig. 3 except over northern South America at 5°N, 65°W.

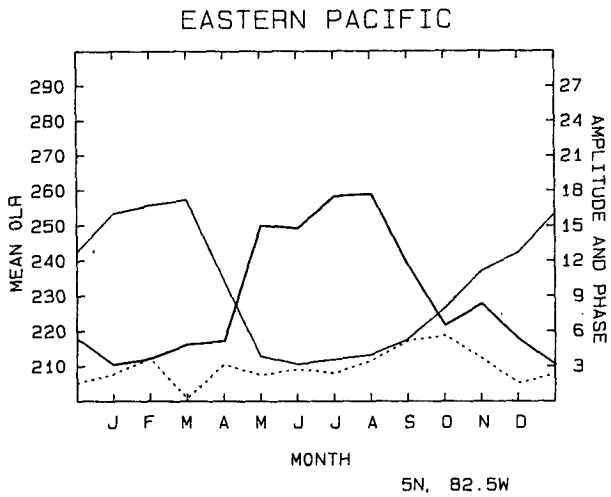

FIG. 12. As in Fig. 3 except over point off west coast of Central America at 5°N, 82.5°W.

nal variation north of Borneo. Gray and Jacobson (1977) found significant diurnal variations in rainfall over small islands, taken to represent the open ocean. Albright et al. (1985) found significant diurnal variations near the equatorial dateline. Likewise, McGarry and Reed (1978) found large diurnal variability in the GATE region of the tropical eastern Atlantic.

Despite the apparently disparate results between our study and others, they are not necessarily inconsistent. Previous studies showed that the diurnal cycle is enhanced during periods of organized activity (Gruber 1976; Gray and Jacobson 1977). Since the data in our study were averaged over both dry and wet regimes, the diurnal cycle is diluted. Second, the oceans exhibit dramatic changes from year to year in the large-scale convection patterns (Liebmann and Hartmann 1982). Again, our averaging over different years means that most areas will experience a dry regime during which the diurnal cycle is reduced (Gray and Jacobson 1977). Also, Hartmann and Recker (1987) and Albright et al. (1985) found that some locations have a significant contribution from the second harmonic, but we have considered only the first harmonic (Gruber and Chen 1988). Finally, studies in the GATE region and off the coast of Borneo (Houze et al. 1981) show the convection to occur in a rather limited area, perhaps too small to be resolved by conventional satellite data. Gray and Jacobson pointed out that the individual cumulonimbus, which undergo significant diurnal variation, cannot be resolved by satellites and the more pervasive cirrus and altostratus decks do not undergo significant diurnal variation.

4. Summary and concluding remarks

There are basically two regimes in which there is a large annual variability of the diurnal cycle. The semiarid regions of the midlatitudes, which are best exemplified by the Middle East and the western United States, exhibit an amplitude of the diurnal cycle which is nearly in phase with the annual cycle of OLR. The maximum emission occurs between 1200 and 1400 throughout the year. This finding is easily explained by considering that during the summer months there is a larger contrast between day and night temperatures in clear, dry areas than during winter. The synoptic systems that penetrate during winter further decrease the amplitude of the diurnal cycle and the mean OLR which increases the summer-winter difference.

The second regime in which one finds a large variability of the diurnal cycle is over those land areas that are characterized by convective cloudiness during summer. Usually the amplitude of the diurnal cycle is largest during the convective season, although there are a few exceptions. At some points over India the amplitude of the diurnal cycle is a minimum during the summer monsoon, and at many locations it decreases during the course of the monsoon. We believe that the minimum in the diurnal cycle during the rainy season results from the persistent large amount of cloudiness present during the rainy season. Since it is rarely clear, the amplitude of the diurnal cycle is reduced. The time of maximum emisssion shifts from between 1200 and 1500 during the dry season (just as it is over the deserts) to between 0600 and 0900 during the convective season.

The amplitude of the diurnal vector increases over India as the dry season progresses. This results, we believe, from a drying of the land to more desert-like conditions with the accompanying large diurnal cycle. Over southern Africa the amplitude of the diurnal cycle also increases as the dry season progresses, and farther south the amplitude during the dry season is larger than during the convective season. The regions of large-scale convection over the ocean exhibit a small diurnal cycle relative to that over land.

We hypothesize a relationship between the standard deviation of OLR and that of the diurnal vector. A visual comparison reveals the large-scale patterns to be related, but the correlation between the two fields is only marginally statistically significant.

The diurnal vector standard deviation pattern is of much smaller scale than the standard deviation of OLR. Evidence of the different scales of the two fields is given by the larger amount of variance explained by 20 harmonics in the standard deviation of OLR field (Fig. 2) than in the diurnal variation field (Fig. 1a). The day–night differences used to calculate the diurnal cycle make the diurnal cycle standard deviation more noisy than the standard deviation of mean OLR itself. The variation of the diurnal cycle is probably also sensitive to a complicated combination of geography, vegetation, and available moisture as well as the large-scale circulation patterns. For example, two areas may both receive little precipitation during a certain season, but a sparsely vegetated region will heat more rapidly dur-

ing the day than a forest, thus producing a different diurnal cycle. Another possible explanation of the small-scale features found in convective regimes is that while the mean OLR is primarily controlled by the mean cloudiness, the diurnal cycle may increase through a certain degree of cloudiness, but once the cloudiness becomes so widespread and persistent that it is present at all times, the diurnal cycle begins to decrease. The standard deviation of monthly mean OLR, on the other hand, is only affected by the largest scales of cloudiness. On regional scales the cloud cover during the convective season may not be persistent enough to result in a strong minimum of mean OLR during that season, thereby resulting in a small standard deviation.

Acknowledgments. We wish to offer thanks to Steven Sotack and M. Chelliah for their assistance with the graphics, and to Larry Stowe and H.M. van den Dool for critical readings of the manuscript. Both reviewers also had worthwhile comments.

The research was performed at the University of Maryland under NOAA grant NA 84-AA-H-00026. Revision of the manuscript took place by the first author at the Cooperative Institute for Research in Environmental Sciences, University of Colorado.

REFERENCES

Albright, M. D., E. E. Recker, R. J. Reed and R. Dang, 1985: The diurnal variation of deep convection and inferred precipitation in the central tropical Pacific during January-February 1979. *Mon. Wea. Rev.*, **113**, 1663–1680.

Aleman, P. A. M., and E. Garcia, 1974: *The Climate of Mexico. World Survey of Climatology, Vol. 11—Climates of North America.* R. A. Bryson and F. K. Hare, Eds., Elsevier Scientific, 345–404.

Brooks, C. E. P., and N. Carruthers, 1953: *Handbook of Statistical Methods in Meteorology.* London, Her Majesty's Stationary Office, 412 pp.

Duvel, J. P., and R. S. Kandel, 1985: Regional-scale diurnal variations of outgoing infrared radiation observed by METEOSAT. *J. Climate Appl. Meteor.*, **24**, 335–349.

Gray, W. M., and R. W. Jacobson, Jr., 1977: Diurnal variation of deep cumulus convection. *Mon. Wea. Rev.*, **105**, 1171–1188.

Gruber, A., 1976: An estimate of the daily variation of cloudiness over the GATE A/B area. *Mon. Wea. Rev.*, **104**, 1036–1039.

Gruber, A., and T. S. Chen, 1987: Diurnal variation of outgoing longwave radiation. *J. Climatol.*, **8**, 1–16.

Hartmann, D. L., and E. E. Recker, 1986: Diurnal variation of outgoing radiation in the tropics. *J. Climate Appl. Meteor.*, **25**, 800–812.

Houze, R. A., Jr., S. G. Geotis, F. D. Marks, Jr. and A. K. West, 1981: Winter monsoon convection in the vicinity of North Borneo. Part I: Structure and time variation of the clouds and precipitation. *Mon. Wea. Rev.*, **109**, 1595–1614.

Kendrew, W.G., 1961: *The Climates of the Continents.* Oxford University Press, 608 pp.

Liebmann, B., and D. L. Hartmann, 1982: Interannual variations of outgoing IR associated with tropical circulation changes during 1974–78. *J. Atmos. Sci.*, **39**, 1153–1162.

Liebmann, B., 1987: Observed relationships between large-scale tropical convection and the tropical circulation on subseasonal time scales during Northern Hemisphere winter. *J. Atmos. Sci.*, **44**, 2543–2561.

McGarry, M. M., and R. J. Reed, 1978: Diurnal variations in convective activity and precipitation during phases II and III of GATE. *Mon. Wea. Rev.*, **106**, 101–113.

Ratisbona, L. R., 1976: *The Climate of Brazil. World Survey of Climatology, Vol. 12—climates of Central and South America.* W. Schwerdfeger, Ed., Elsevier Scientific, 219–293.

Reed, R. J., and K. D. Jaffe, 1981: Diurnal variation of summer convection over West Africa and the tropical eastern Atlantic during 1974 and 1978. *Mon. Wea. Rev.*, **109**, 2527–2534.